

Bright X-ray source populations in the starburst galaxies NGC 4038/4039

Xi-Wei Liu and Xiang-Dong Li

Department of Astronomy, Nanjing University, Nanjing 210093, China

Received ; accepted

Abstract Assuming a naive star formation history, we construct the synthetic X-ray source populations for comparison with the X-ray luminosity function (XLF) of the interacting galaxies NGC 4038/4039 using a population synthesis code. We have considered high- and intermediate-mass X-ray binaries, young rotation-powered pulsars and fallback disk-fed black holes in modeling the bright X-ray sources detected. We find that the majority of the X-ray sources are likely to be intermediate-mass X-ray binaries, but for typical binary evolution parameters, the predicted XLF seems to be steeper than observed. We note that the shape of the XLFs depends critically on the existence of XLF break for young populations, and suggest super-Eddington accretion luminosities or the existence of intermediate-mass black holes to account for the high luminosity end and the slope of the XLF in NGC 4038/4039.

Key words: binaries: close — galaxies: individual (NGC 4038/4039) — stars: evolution — X-ray: binaries

1 INTRODUCTION

With *Chandra*'s unprecedented sensitivity and angular resolution, populations of individual X-ray sources, with luminosities comparable to those of Galactic X-ray binaries, can be detected at the distance of the Virgo Cluster and beyond (Fabbiano 2006). *Chandra* observations of the merging galaxies NGC 4038/4039 (the Antennae) provide a unique opportunity for the study of the X-ray source populations in young and intense starburst environments (Fabbiano, Zezas & Murray 2001; Zezas et al. 2002a, 2002b; Zezas &

★ E-mail: liuxw@nju.edu.cn, lixd@nju.edu.cn

Fabbiano 2002, hereafter ZF02). Among the 43 point-like sources detected by *Chandra* (down to a limiting luminosity of $\sim 10^{38} \text{ erg s}^{-1}$), 17 sources have inferred luminosities above $\sim 10^{39} \text{ erg s}^{-1}$, assuming an isotropic emission. These luminosities exceed the Eddington limit of a $10 M_{\odot}$ accreting black hole (BH), and we classified these sources as ultraluminous X-ray sources (ULXs). Although accretion binaries with a BH of mass in the range $100 - 1000 M_{\odot}$ (i.e., intermediate mass black holes, IMBHs) can easily explain these super-Eddington luminosities, they may not account for the majority of the ULXs in the Antennae galaxies (ZF02). One possible explanation is that the X-ray radiation of the ULXs is not isotropic, so the real luminosities are much lower the inferred values (King et al. 2001). Alternatively, Begelman (2002) suggested that in radiation-dominated accretion disks, the radiation could escape from the disk (due to photon bubble instability) at a rate higher than predicted by the standard accretion disk theory, so that the escaping flux could exceed the Eddington luminosity by a factor of up to $\sim 10 - 100$. ZF02 and Zezas et al. (2007) derived the X-ray luminosity function (XLF) of the X-ray source populations in the Antennae. The cumulative XLF is well fit by a power-law with an index of $\sim 0.5 - 0.8$, consistent with (though slightly flatter than) the slope of the “universal luminosity function” for the HMXB populations in various types of galaxies (Grimm, Gilfanov & Sunyaev 2003). Here, we model the observed XLF (with both the shape and the absolute source number) by using evolutionary population synthesis (EPS) method, to evaluate the effects of the input parameters on the calculated results. Although there have been many observations of the point X-ray sources in external galaxies, theoretical investigations on the X-ray source populations remain to be limited. Ghosh & White (2001) discussed the evolution of X-ray luminosities of normal galaxies with the cosmological evolution of the star formation rate (SFR) in a semi-numerical fashion. Wu (2001) constructed an analytic model and calculated the luminosity function of X-ray binaries in external galaxies. Both of them have adopted simple assumptions on the formation and evolution of X-ray binaries. A recent population synthesis study on the XLF of NGC 1569 was done by Belczynski et al. (2004).

This paper is organized as follows. In §2 we describe the population synthesis method and the models for various types of X-ray sources. The calculated results are presented in §3. Discussion and conclusions are in §4.

2 MODEL DESCRIPTION

2.1 Method and input parameters

We use the EPS code developed by Hurley, Pols, & Tout (2000) and Hurley, Tout, & Pols (2002, hereafter HTP02) to calculate the expected numbers and X-ray luminosity distributions in the Antennae for various types of single and binary X-ray source populations. This code incorporates the evolution of single stars with binary star interactions, such

as mass transfer, mass accretion, common-envelope (CE) evolution, collisions, supernova (SN) kicks, tidal friction and angular momentum loss mechanisms (i.e. mass loss, magnetic braking and gravitational radiation). In this work, we have modified the EPS code so that it can perform better in simulating binary evolution in a variety of circumstances (see appendix).

We start with the parameters input into the code for population synthesis. We assume a fraction f ($0 < f < 1$) of stars are born in binaries. Surveys of M dwarfs within 20 pc from the Sun have suggested that f may be a function of stellar spectral types (Fischer & Marcy 1992). According to recent works on stellar multiplicity (Lada 2006; Kobulnicky, Fryer & Kiminki 2006, hereafter KFK06), stars with later spectral types are more likely single, for example, $f > 50\%$ for G stars, and $f > 0.6$ (in the most probable range $0.7 < f < 0.85$) for massive O/B stars in the Cygnus OB2 association surveyed by KFK06. We have adopted $f = 0.5$ or 0.8 in our calculations. The initial mass function (IMF) of Kroupa, Tout, & Gilmore (1993, hereafter KTG93) is taken for the primary's mass (M_1) distribution. For the secondary stars (of mass M_2), in our standard model we assume uniform distributions of the mass ratio $q = M_2/M_1$ between 0 and 1 and of the logarithm of the orbital separation ($\ln a$). However, KFK06 suggested more general power-law distributions of the secondary masses and orbital separations, i.e., $P(q) \propto q^\alpha$ and $P(\ln a) \propto (\ln a)^\beta$, where the power-law indices $\alpha > 0$ and $-2 < \beta < 0.5$. We have designed several models to examine the effects of changing these primordial binary parameters (f , α and β) on the results.

Reliable inputs for the SFR and star formation history (SFH) are crucial to population synthesis of the X-ray sources detected in the Antennae galaxies. For the SFR we adopt the value of $7.1 M_\odot \text{yr}^{-1}$ for stars more massive than $5 M_\odot$ (Grimm, Gilfanov & Sunyaev 2003), which was obtained based on the measurement of several canonical indicators of SFR, namely UV, $\text{H}\alpha$, FIR and thermal radio emission fluxes. This value was then converted into the specific SFRs S_s and S_b used in the EPS code. Here S_s and S_b (in unit of yr^{-1}) denote the formation rates of single and binary star populations, respectively. Since the binary fraction is f , we have

$$\frac{2S_b}{S_s + 2S_b} = f. \quad (1)$$

The amount of mass produced per year in stars more massive than $5 M_\odot$ is

$$S_b \int_5^\infty m_1 \xi(m_1) dm_1 + S_b \int_5^\infty \xi(m_1) \left(\int_5^{m_1} \frac{m_2}{m_1} dm_2 \right) dm_1 + S_s \int_5^\infty m \xi(m) dm = 7.1, \quad (2)$$

where $\xi(m)$ is the IMF. The first and second terms on the left-hand-side of Eq. (2) represent the amount of mass formed per year as the primary and secondary star of a binary, respectively. Contribution from single stars is evaluated in the third term.

Combining Eqs. (1) and (2), we have

$$S_s = \frac{14.2 - 14.2f}{0.144 - 0.045f} \text{ and } S_b = \frac{7.1f}{0.144 - 0.045f}. \quad (3)$$

The values of the single and binary star SFRs can be input into the single stellar evolution (SSE) and binary stellar evolution (BSE) code, respectively (see §4.1 of HTP02 for details). For a binary fraction $f = 0.5$, we get $S_s = 58.4 \text{ yr}^{-1}$ and $S_b = 29.2 \text{ yr}^{-1}$.

According to current models on the evolution of the Antennae, closest passage of the two galaxies comprising the Antennae happened roughly 200 Myrs ago (Barnes 1988; Mihos, Bothun & Richstone 1993). The merging induced star formation tends to persist for 0.5 to 1 dynamical time (i.e., the orbital time-scale of the last encounter) (Mengel et al. 2005). It is expected that most of the X-ray sources detected are relatively young objects produced after the merging process, so we adopt a naive model for the SFH that assumes the Antennae have been keeping the current SFR for the last 300 or 100 Myr. Since we are concerned with young populations, we do not take the SFH earlier into account.

2.2 Models for X-ray sources

We consider three types of X-ray source populations for the X-ray sources detected in the Antennae.

A large fraction of the X-ray sources should be X-ray binaries containing accreting neutron stars (NSs) or BHs. For starburst galaxies like the Antennae, high-mass X-ray binaries (HMXBs) with the secondary masses $M_2 > 8 M_\odot$ and intermediate-mass X-ray binaries (IMXBs) with $2 M_\odot < M_2 < 8 M_\odot$ are the most natural explanation for the bright point-like sources in these galaxies (low-mass X-ray binaries are too old for our assumed SFH). According to the manner of the accretion onto the accretor (NSs or BHs), X-ray binaries can be divided into two classes, i.e., wind-accreting (WA) and Roche-lobe overflow (RLOF) systems. In the former case we adopt the standard Bondi & Hoyle (1944) wind-accretion formula to calculate the mass accretion rate of the NSs/BHs. The velocity v_W of the winds from the massive donor stars is taken to be $v_W = \sqrt{2\beta(GM_2/R_2)}$, where R_2 is the radius of the donor star, and the value of β depends on the spectral type of the stars. HTP02 suggested it is in the range of 0.125 – 7.0. The gravitational energy released by the accreted material is converted into radiation, and we have to correct the calculated bolometric luminosities into those in the *Chandra* detection band of 0.1 – 10 keV. Since the WA NS systems have relatively hard spectra that can be described with a $\Gamma \sim 0$ power law below 10 keV (e.g. Campana et al. 2001), we assume that almost all the radiation energy is concentrated in the *Chandra* band, and no bolometric correction is needed. For the other RLOF X-ray binaries we adopt a correction factor of 0.5.

Current stellar evolution models predict that during the core collapse of massive stars, a considerable amount of the stellar material will fall back onto the compact,

collapsed remnants (NSs or BHs), usually in the form of an accretion disk. Li (2003) suggested that some of the ULXs in nearby galaxies, which are associated with supernova remnants, may be BHs accreting from their fallback disks. Not all natal BHs can possess a fallback disk, unless the BH progenitors have enough angular momentum to form a centrifugally supported disk. The condition that matter does not spiral into the BH at the onset of collapse is that the rotational energy of the matter should be greater than half the gravitational potential energy (Izzard, Ramirez-Ruiz & Tout 2004): $J^2/(2I) \geq GM_{\text{BH}}m/(2r_{\text{LSO}})$, where J is the angular momentum of the matter, $I = mr_{\text{LSO}}^2$ is its moment of inertia and r_{LSO} is the radius of the last stable orbit (LSO) around a BH. In fact for Population I ($Z = 0.02$) stars, from our calculations only those in close binaries can be spun up so fast (due to spin-orbit tidal evolution) that fallback disks can form after core collapse. After an initial transient phase of duration t_0 , the disk mass M_d , outer radius R_d , and mass accretion rate \dot{M}_d obey the simple power-law evolution, i.e. $M_d \propto t^{-p}$, $R_d \propto t^{2p}$ and $\dot{M}_d \propto t^{-(1+p)}$ (Cannizzo, Lee & Goodman 1990), and we adopt $p = 3/16$ in this paper. Menou, Perna & Hernquist (2001, hereafter MPH01) argued that the power-law evolution breaks down when the disk is cool enough to become neutral. We thus limit our calculation on the disk evolution to the neutralization time t_n . Following MPH01 we derived the time t_n to be

$$t_n \simeq 6.6 \times 10^{\frac{12-35p}{1+7p}} R_8(t_0)^{\frac{7p-6}{2+14p}} \left[\frac{M_d(t_0)}{10^{-3}M_\odot} \right]^{\frac{1}{1+7p}} T_{c,6}^{-\frac{7p}{1+7p}} \text{ yr}, \quad (4)$$

where $R_8(t_0)$ is the initial radius of the disk in units of 10^8 cm, and $T_{c,6}$ the typical temperature of the disk during the initial transient phase in units of 10^6 K. Here we adopt $R_8(t_0) = 1$, and $T_{c,6} = 1$. For $M_d(t_0)$ we assume a uniform distribution of $\log M_d(t_0)$ in the range of $10^{-5} - 1 M_\odot$. The bolometric correction factor of the fallback disk-fed systems is also chosen to be 0.5.

Moreover, the X-ray emission from accreting compact stars (both single and in binaries) is generally assumed to be isotropic. However, for disk accreting sources, the geometric effect may affect the apparent luminosity distributions (Zhang 2005). For the RLOF X-ray binaries and the fallback disk-fed BHs we have taken into account the geometric effect in calculating their X-ray luminosities (see also Liu & Li 2006).

Rotation-powered pulsars also shine in X-rays. There appears to be a strong correlation between the rates of rotational energy loss \dot{E} and their X-ray luminosities L_X (Seward & Wang 1988; Becker & Trumper 1997; Possenti et al. 2002). Generally younger pulsars have stronger X-ray emission. Perna & Stella (2004) argued that a fraction of ULXs could be young, Crab-like pulsars, especially starburst galaxies should each have several of these sources, and the X-ray luminosity of a few percent of galaxies is dominated by a single bright pulsar with $L_X \geq 10^{39} \text{ ergs}^{-1}$, roughly independent of its SFR. Following Perna & Stella (2004) and Liu & Li (2006) we adopt the empirical relation by Possenti et al. (2002) to estimate the 2 – 10 keV X-ray luminosities of young pulsars.

To our knowledge this work is the first to include all the three types of X-ray source populations suggested in the literature in modeling the XLF of external galaxies.

3 RESULTS

We have adopted a variety of models with different assumptions for the input parameters (see Table 1). We set Model 1 (hereafter M1) as the control model, while other models are designed to test the effects of the input parameters. In Fig. 1 we show the calculated XLF in M1, and the components contributed by HMXBs, IMXBs, fallback disk sources, and pulsars in the Antennae. One can see that IMXBs dominate the total X-ray luminosity range, and young pulsars also contribute a few of the brightest sources. HMXBs play a minor role in the total population due to their relatively short lifetime compared to IMXBs. Fallback disk sources are much fewer than the above three classes of sources. The break at $\sim 4 \times 10^{38} \text{ ergs}^{-1}$ is caused by the Eddington luminosity of accreting BHs.

A comparison of the calculated and measured XLFs is shown in Fig. 2. Obviously the model predicts more X-ray sources at luminosities $L_x < 5 \times 10^{38} \text{ ergs}^{-1}$, but less when $L_x > 5 \times 10^{38} \text{ ergs}^{-1}$. Especially the break in the XLF makes it considerably steeper than observed. We note that the XLF breaks for young populations seem to be a general feature predicted in theoretical works (e.g. Wu 2001; Fig. 1 of Belczynski et al. 2004; Fig. 6 of Rappaport et al. 2005). Consider that the young X-ray populations have relatively flat XLF (Grimm et al. 2003), the analysis on the difference in the modeled and observational XLFs should not only be limited to the Antennae, but may have a more general application.

The shape of the XLF was suggested to be related to the star formation activity (Wu 2001) and to the NS/BH mass spectrum and the mass transfer rates in binary stars (Grimm et al. 2003). We will check these points in the following. There are large uncertainties in estimating the SFH and SFR in the Antennae. Obviously, shorter SFH leads to smaller number of XRBs, but decreasing the duration of star formation in the Antennae seems not affect the XLF considerably. For example, if the SFH is changed from 300 Myr to 100 Myr, the lower end of the XLF is down by a factor of ~ 40 , while the higher end changes little. If we take half of the adopted SFR (model M3), however, the number of the X-ray sources with $L_x < 5 \times 10^{38} \text{ ergs}^{-1}$ can be significantly decreased to be compatible with observations. This is easily understood, since the formation of H/IMXBs is closely correlated with the global SFR. Alternatively, the same effect can be reached if we lower the binary fraction from 50% in M1 to 10% (model M2). This is also reasonable, since, if most of the X-ray binaries originate from the star clusters in the Antennae (Zezas et al. 2002b), those ejected from the clusters usually have relatively high space velocities, and are more likely to be disrupted due to SN kick (Belczynski et al. 2006). The third way to reduce the number of H/IMXBs is to decrease the CE parameter

η_{CE} . In model M4, η_{CE} is set to be 0.1, much smaller than unity usually adopted, the mass ratio q and orbital separation $\ln a$ distributions are taken to be q^1 and $(\ln a)^{-1}$, respectively. These factors can significantly decrease the number of IMXBs - the peculiar q and $\ln a$ distributions cause a bias toward the formation of narrow HMXBs, while small η_{CE} leads to coalescence of the progenitors of IMXBs. The resulting XLF does not show any prominent break since the XLF is now dominated by young pulsars and the fallback disk sources. This feature can be tested by future multi-wavelength observations.

However, even with the above modifications, the high end of the XLF, which plays a critical role in determining the slope of the XLF, is still not accounted for (see Fig. 2). Our calculations show that it hardly depends on the IMF (Stolte et al. 2002), distributions of the mass ratio or orbital separation, and the metallicity.

Figure 1 clearly suggests that the slope of XLF critically depends on the Eddington luminosities of BHs in IMXBs. In M1 the actual maximum luminosities of accreting BHs and NSs are taken to be 10 times the corresponding Eddington luminosities. It has been pointed out that these values can be as high as ~ 100 if the accretion rates are very high in the cases of H/IMXBs (Belgelman 2002). In models M2 and M4, we further increase the super-Eddington factor from 10 to 100, and the XLF correspondingly extends to $\lesssim 10^{40}$ ergs $^{-1}$. The modeled XLFs discussed above are demonstrated in Fig. 2, in comparison with the observed XLF. The solid, dashed, dot-dashed, and dotted lines represents the results of models M1-M4, respectively.

4 DISCUSSIONS

We have performed population synthesis calculations to explore the possibility of reproducing the observed XLF in the Antennae with current understanding of formation and evolution of compact stars. According to our calculations, there are two parameters which affect the XLF most prominently: the binary formation rate and the factor of super-Eddington accretion rate allowed. The former parameter, depending on the global SFR and IMF, the binary fraction and interactions, determines the overall number of the X-ray sources and the mass spectrum of compact stars. The latter is related to the accretion behavior, and constrains the location of the break in the XLF. They jointly design the shape of the XLF. For the Antennae we conclude that the majority of the luminous X-ray sources are likely to be IMXBs, but their formation should be strongly influenced by star formation activity and binary interactions. Zezas et al. (2002b) showed that the position of most of the Antennae sources is near but *not* coincident with optical young clusters (with typical offsets $\sim 100 - 300$ pc). Assuming that this displacement is caused by the motion due to supernova kicks, these authors suggested that most of the X-ray sources may be accreting NS/BH binaries with donor stars of masses ranging from 2 to $10 M_{\odot}$. This inference is consistent with our result that IMXBs dominate the

XLF in the standard model M1 (see Fig. 1). However, the XLF in the model shows a clear break at a few $10^{38} \text{ erg s}^{-1}$, which is related to the Eddington luminosities of accreting BHs. This makes the XLF steeper in the ULX luminosity range ($> 10^{39} \text{ erg s}^{-1}$) than the observational one, although the latter is subject to small number statistics and large observational uncertainties. There is also evidence for the breaks in the XLFs for other nearby galaxies (e.g. Sarazin et al. 2000; Shirey et al. 2001). However, the break luminosities are still unclear because of the distance uncertainties. We find that super-Eddington X-ray luminosities are required to account for the flat XLF extending to $\sim 10^{40} \text{ erg s}^{-1}$. Theoretically it has been realized that rapid mass accretion is more likely to occur in IMXBs than in LMXBs, where mass transfer proceeds on thermal rather nuclear timescale. It is also in accord with the strong correlation found between the number and average luminosity of ULXs in spirals and their host galaxies far-infrared luminosity (Swartz et al. 2004). Alternatively, some of the most luminous X-ray sources in the Antennae could be IMBHs. Only a few these objects can interpret the “overabundance” of the high luminosity end of the XLF. The available observations are not able to present stringent constraints on the nature of these X-ray sources, and rule out the possibility of IMXBs in the Antennae.

Tennant (2001) firstly identified the two different types of XLF in the Galactic disk and bulge: the XLF of the disk follows a power law with an index ~ 0.5 and that of the bulge follows a similar shape but with a steeper slope. Kilgard et al. (2002) showed that the XLF slope is correlated with the age of the X-ray binary populations, and the XLFs of starburst galaxies with relatively more luminous sources are flatter than those of spiral galaxies. Wu (2001) constructed a birth-death model and calculated the XLF of X-ray binaries in external galaxies. It was found that the location of the break in the XLF depends on the look-back time of the previous starburst activity, and no break appears if there is no starburst (as for the disk sources in M81). In Kilgard et al. (2002), all of the X-ray sources were assumed to be members of a single population with uniform properties except for luminosity and lifetime. The actual situation may be much more complicated. For example, IMXBs generally form later than HMXBs after the starburst, but they can be much more brighter than wind-fed HMXBs when RLOF occurs. This mixed formation sequences of various types of X-ray binaries could produce “ripples” rather a uniformly evolving break in the XLF. This conclusion is only for the young X-ray populations (with age $< 300 \text{ Myr}$). Since we do not consider low-mass X-ray binaries, we cannot evaluate the long-term ($\sim \text{Gyr}$) effect of starburst here. It is possible that there exists a uniformly break evolution in the XLF of old stellar populations (e.g. Kong et al. 2002).

Our population synthesis study is obviously subject to many uncertainties. Little are known about not only the detail SFR, SFH, and IMF in the Antennae, but also some key processes, for example, the CE evolution, in the formation and evolution of X-ray binaries. Estimation of the X-ray luminosities is also influenced by the detailed accretion modes

in X-ray binaries. Finally, It should be emphasized that the calculated mass transfer rates (and the X-ray luminosities) are long-term, averaged ones. It is unclear how to relate these secular mass transfer rates to observable instantaneous X-ray luminosities. More detailed X-ray observations of a large sample of galaxies across the full Hubble sequence are required to determine the nature of the break luminosities in the XLF and the XLF evolution. These observations, coupled with development of stellar and binary evolution models, may provide new insights into the compact object populations in external galaxies.

Acknowledgements We would like to thank Jarrod R. Hurley for kindly providing us the SSE and BSE codes and valuable conversations. We are grateful to an anonymous referee for a number of insightful remarks, and Yang Chen, Hai-Lang Dai, Wen-Cong Chen and Zhao-Yu Zuo for useful discussions. This work was supported by Natural Science Foundation of China under grant numbers 10573010 and 10221001.

References

- Barnes J. E. 1988, *ApJ*, 331, 699
 Becker W., Trumper J. 1997, *A&A*, 326, 682
 Begelman M. C. 2002, *ApJ*, 568, L97
 Belczynski K., Dalogera A., Zezas A. & Fabbiano G. 2004, *ApJ*, 601, L147
 Belczynski K., Sadowski, A., Rasio F. A. 2004, *ApJ*, 611, 1068
 Belczynski K., Sadowski A., Rasio F. A., Bulik, T. 2006, *ApJ*, 650, 303
 Belczynski K., Taam, R. E. 2004, *ApJ*, 616, 1159
 Bondi H., Hoyle F. 1944, *MNRAS*, 104, 273
 Cannizzo J. K., Lee H. M., Goodman J. 1990, *ApJ*, 351, 38
 Campana S. et al. 2001, *ApJ*, 561, 924
 Fabbiano G. 2006, *ARA&A*, 44, 323
 Fabbiano G., Zezas A., Murray S. 2001, *ApJ*, 554, 1035
 Fischer D. A., Marcy G. W. 1992, *ApJ*, 396, 178
 Fryer C. L. 1999, *ApJ*, 522, 413
 Grimm H.-J., Gilfanov M., Sunyaev R. 2003, *MNRAS*, 339, 793
 Hobbs G., Lorimer D. R., Lyne A. G., Kramer M. 2005, *MNRAS*, 360, 963
 Hurley J. R., Pols O. R., Tout C. A. 2000, *MNRAS*, 315, 543
 Hurley J. R., Tout C. A., Pols O. R. 2002, *MNRAS*, 329, 897
 Izzard R. G., Ramirez-Ruiz E., Tout C. A. 2004, *MNRAS*, 348, 1215
 Kilgard R. E. et al. 2002, *ApJ*, 573, 138
 Kobulnicky H. A., Fryer C. L., Kiminki D. C. 2006, submitted to *ApJ*, astro-ph/0605069
 Kong A. K. H. et al. 2002, *ApJ*, 577, 738
 Kroupa P., Tout C. A., Gilmore G., 1993, *MNRAS*, 262, 545, KTG93
 Lada C. J. 2006, *ApJ*, 640, L63
 Li X. D. 2003, *ApJ*, 596, L199
 Liu X. W., Li X. D. 2006, *A&A*, 449, 135
 Mengel S., Lehnert M. D., Thatte N., Genzel R. 2005, *A&A*, 443, 41
 Menou K., Perna R., Hernquist L. 2001, *ApJ*, 559, 1032
 Mihos J. C., Bothun G. D., Richstone D. O. 1993, *ApJ*, 418, 82
 Perna R., Stella L. 2004, *ApJ*, 615, 222
 Possenti A., Cerutti R., Colpi M., Mereghetti S. 2002, *A&A*, 387, 993
 Rappaport S. A., Podsiadlowski Ph., Pfahl E. 2005, *MNRAS*, 356, 401

- Remillard R. A., McClintock J. E. 2006, *ARA&A*, 44, 49
- Salpeter E. E. 1955, *ApJ*, 121, 161
- Sarazin C. L., Irwin J. A., Bregman J. N. 2000, *ApJ*, 544, L101
- Seward F. D., Wang Z. 1988, *ApJ*, 332, 199
- Shirey R. et al. 2001, *A&A*, 365, L195
- Stolte A., Grebel E. K., Brandner W., Figer D. F. 2002, *A&A*, 394, 459
- Swartz, D. A., Ghosh K. K., Tennant A. F., Wu K. 2004, *ApJS*, 154, 519
- Tennant A. F., Wu K., Ghosh K. K., Kolodziejczak J. J., Swartz D. A. 2001, *ApJ*, 549, L43
- Wu K. 2001, *PASA*, 18, 443
- Zezas A., Fabbiano G. 2002, *ApJ*, 577, 726
- Zezas A., Fabbiano G., Rots A. H., Murray S. S. 2002a, *ApJS*, 142, 239
- Zezas A., Fabbiano G., Rots A. H., Murray S. S. 2002b, *ApJ*, 577, 710
- Zezas A. et al. 2007, *ApJ* preprint (doi:10.1086/‘513091’)
- Zhang S. N. 2005, *ApJ*, 618, L79

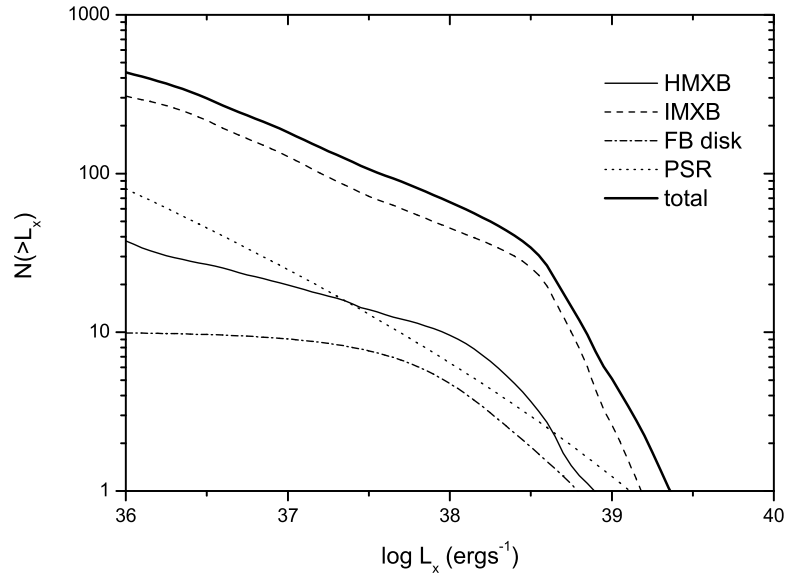


Fig. 1 The XLFs and its components in model M1.

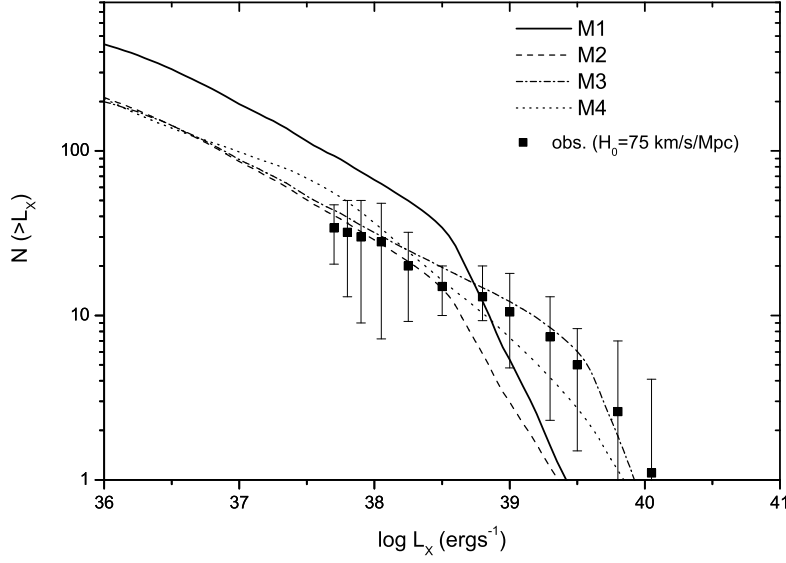


Fig. 2 Comparisons of the modeled and observed XLFs. M1 is the standard model. Compared with M1, in M2 the binary fraction is decreased by a factor of 5, in M3 the SFR is decreased by a factor of 2, and the factor for super-Eddington accretion rate increased by a factor of 10 (note that the XLF in M2 can also extend to $\sim 10^{40} \text{ ergs}^{-1}$ if the latter assumption is adopted). In M4 we take the value of the CE parameter $\eta = 0.1$ and atypical distributions of mass ratio and orbital separation.

Table 1 Model Parameters.

Model	η	SFR ($M_{\odot}\text{yr}^{-1}$)	f	$P(q)$	$P(\ln a)$	Edd
M1	1.0	7.1	0.5	$\propto q^0$	$\propto (\ln a)^0$	10
M2	1.0	7.1	0.1	$\propto q^0$	$\propto (\ln a)^0$	10
M3	1.0	3.5	0.5	$\propto q^0$	$\propto (\ln a)^0$	100
M4	0.1	7.1	0.8	$\propto q^1$	$\propto (\ln a)^{-1}$	100

Note: η - the CE efficiency parameter; SFR - the SFR for stars massive than $5 M_{\odot}$; f - initial binary fraction; q - initial mass ratio; a - initial orbital separation; Edd - the factor of super-Eddington accretion rate allowed.

Appendix A: MODIFICATIONS TO THE ORIGINAL EPS CODE

Firstly, the original EPS code produces BHs with unreasonable low masses. In Fig. A1 we show the masses of the stellar remnants (i.e. compact objects) as a function of the masses of their zero-age main sequence (ZAMS) stars. The BH masses are determined by an empirical function of the Carbon-Oxygen core masses of the pre-collapse progenitor stars, i.e. $m_{\text{BH}} = 1.17 + 0.09m_{\text{co}}$. In the top panel of Fig. A1 we show the calculated results with the original code. We note that the natal BH masses are in a narrow range of $\sim 1.8 - 2.0 M_{\odot}$, which are significantly smaller than those ($\sim 3 - 18 M_{\odot}$) of the observed BH candidates in our Galaxy (Remillard & McClintock 2006). We have modified the empirical formula in the code to be $m_{\text{BH}} = -33 + 6m_{\text{co}}$, so that a larger range of BH masses ($\sim 4 - 10 M_{\odot}$ and $\sim 5 - 26 M_{\odot}$ for population I and II stars respectively) can be produced, which are shown in the middle and lower panels. The figure illustrates that the lower limits for the BH progenitor masses are $\sim 23 M_{\odot}$ ($Z = 0.02$) and $\sim 20 M_{\odot}$ ($Z = 0.001$), consistent with the putative values (e.g. Fryer 1999). It is noted that similar modification was made by Belczynski, Sadowski & Rasio (2004).

Secondly, the EPS code assumes that all non-compact stars suffer magnetic braking if it is more massive than $0.35 M_{\odot}$. However, stars more massive than $1.5 M_{\odot}$ have radiative envelopes which cannot generate strong magnetic field. So we taken into account the magnetic braking mechanism only for stars of $M < 1.5 M_{\odot}$. Thirdly, when a main sequence star overfills its Roche lobe and is 2.5 times more massive than its companion (the accretor), a very rapid, dynamically unstable mass transfer phase would emerge, and the orbital separation would decline dramatically. We thus assume the binary would coalescence, and no further calculation is taken.

The fourth modification is about the natal BH kick velocities. During the SN explosions, a kick velocity v_{k} is imparted on the newborn compact stars with the Maxwellian distribution

$$P(v_{\text{k}}) = \sqrt{\frac{2}{\pi}} \frac{v_{\text{k}}^2}{\sigma^3} \exp\left(-\frac{v_{\text{k}}^2}{2\sigma^2}\right) \quad (\text{A.1})$$

where $\sigma = 265 \text{ kms}^{-1}$ for neutron stars (NSs) (Hobbs et al. 2005). We assume that only those BHs experienced SN explosions would be imparted on a natal kick velocity, which is inversely proportional to the BH mass, i.e. $v_{\text{kick,BH}} = 1.4/M_{\text{BH}} \times v_{\text{kick,NS}}$. Apart from core collapse SNe, Belczynski & Taam (2004) suggested the formation of NSs via accretion-induced collapse of massive white dwarfs. We do not take it into account due to the large uncertainties of the AIC assumption.

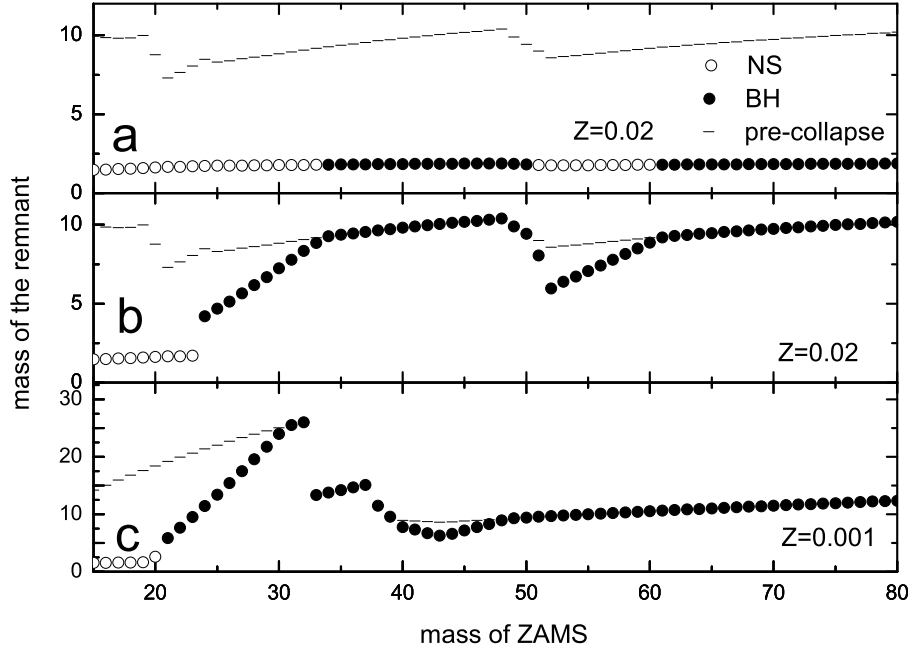


Fig. A.1 Final remnant (NS/BH) masses as a function of ZAMS progenitor mass for different metallicities. The top panel shows the calculated result with the original BSE code, the middle and bottom panels show those with our modified code.